Computer-Aided Design ▮ (▮▮▮▮) ▮▮▮–▮▮▮

Contents lists available at ScienceDirect

Computer-Aided Design

journal homepage: www.elsevier.com/locate/cad

Curvature-aware adaptive re-sampling for point-sampled geometry

Yongwei Miao [a,b,c,*], Renato Pajarola [c], Jieqing Feng [a]

[a] State Key Laboratory of CAD&CG, Zhejiang University, China
[b] College of Science, Zhejiang University of Technology, China
[c] Department of Informatics, University of Zurich, Switzerland

ARTICLE INFO

Article history:
Received 14 April 2008
Accepted 22 January 2009

Keywords:
Point-sampled geometry
Adaptive re-sampling
Simplification
Curvature-aware
Mean-shift clustering

ABSTRACT

With the emergence of large-scale point-sampled geometry acquired by high-resolution 3D scanning devices, it has become increasingly important to develop efficient algorithms for processing such models which have abundant geometric details and complex topology in general. As a preprocessing step, surface simplification is important and necessary for the subsequent operations and geometric processing. Owing to adaptive mean-shift clustering scheme, a curvature-aware adaptive re-sampling method is proposed for point-sampled geometry simplification. The generated sampling points are non-uniformly distributed and can account for the local geometric feature in a curvature aware manner, i.e. in the simplified model the sampling points are dense in the high curvature regions, and sparse in the low curvature regions. The proposed method has been implemented and demonstrated by several examples.

1. Introduction

With the rapid development of various 3D scanning devices, point-sampled geometry has become a powerful alternative to the traditional polygonal geometric model in computer graphics [1–3]. Efficient modeling and rendering techniques for the point-sampled geometry have developed into an attractive research area for its potential ability in representing complex geometric models with high-fidelity [4–6]. However, due to the large memory requirement and high time complexity, efficiently processing large scale point-sampled geometry is still facing great challenges, such as storage, editing, transmission, and rendering, etc. To achieve real-time performance required in many application fields such as entertainment, industrial design, virtual reality etc. [7,8], a simplification procedure is an efficient solution to alleviate the storage and time complexities.

In the point-sampled geometry simplification, it is important to choose the representative points and re-sampling the original geometry for faithfully approximating the underlying geometry in both geometry and topology. In practical applications, how to keep geometric features may attract more attentions since it is a comparably simple task to keep the simplified model topology unchanged. Thus, pursuing the geometry fidelity of the simplified model, the sampling density variation should manifest the local geometric features, i.e. the sample points should be dense in the sharp features regions (usually with high curvatures), and sparse in the relative planar regions (usually with low curvatures). Another important issue that relates to surface re-sampling is the theoretical analysis of sampling conditions and other pre-conditions for correct reconstruction of surfaces with or without boundaries [9–11].

Owing to the efficiency of feature space analysis, a mean-shift scheme is performed in both spatial and range domain of the underlying geometry. Due to the bilateral filtering property of our mean-shift clustering scheme, the proposed re-sampling approach can filter moderate noise attached by the given model. Moreover, in order to guide a feature sensitive re-sampling procedure, unlike the fixed bandwidth mean-shift clustering, the proposed adaptive scheme is suitable for the moderately non-uniformly distributed point-sampled geometry. However, point clouds with highly non-uniform sampling or large noise cannot be treated well by our algorithm. For these raw scanner data, some pre-processing steps [12] should be performed for subsequent re-sampling task.

The contributions are summarized as follows:

- Based on an adaptive mean-shift clustering scheme, a novel point-sampled geometry simplification method is proposed, which can adaptively re-sample the underlying model so as to reflect the intrinsic geometry features whilst introducing relatively lower geometric error.
- By choosing different thresholds and different weights in our mean-shift clustering scheme, the adaptive re-sampling scheme can adapt to different sampling density requirements of the underlying point-sampled geometry.

* Corresponding author.
E-mail addresses: miaoyw@cad.zju.edu.cn, ywmiao@zjut.edu.cn (Y. Miao).

0010-4485/$ – see front matter © 2009 Elsevier Ltd. All rights reserved.
doi:10.1016/j.cad.2009.01.006

- Our simplification scheme is time efficient and easy to implement. It allows direct processing of scanned data without the need to construct polygonal meshes beforehand, leading to an increased overall performance.

The paper is organized as follows. The related work on simplification and re-sampling methods for point-sampled geometry is reviewed in Section 2. In Section 3, an adaptive mean-shift scheme is proposed to analyze the local maxima of a multivariate probability density function. Based on the mean-shift analysis, an adaptive re-sampling approach for the point-sampled geometry is described in Section 4. In Section 5, some experimental results are listed and the geometric error analysis by our re-sampling scheme is given. Finally, conclusions are drawn and directions for future research are given in Section 6.

2. Related work

Surface simplification and re-sampling. Many pieces of work related to point-sampled geometry simplification and re-sampling have been proposed in digital geometry processing, such as extrinsic Voronoi diagram-based scheme, intrinsic technique, grid-based and statistical-based approach, incremental and hierarchical clustering scheme, iterative simplification method, and particle-based re-sampling approach, etc.

Dey et al. [13] presented a dedicated point cloud simplification algorithm using the particular structure of 3D Voronoi cells of a dense point cloud. It is a locally restricted method and cannot handle the non-uniformly distributed point clouds or point clouds with holes. Moenning and Dodgson [14,15] presented an intrinsic coarse-to-fine simplification algorithm with sampling density guarantee for point clouds. However, their algorithm requires the complicated computation of intrinsic geodesic Voronoi diagrams. Linsen [2] proposed a point set simplification scheme that associated each input sample point with an information content measure and then iteratively removed points with lowest entropy. This re-sampling algorithm is only limited to the generation of point cloud subsets and cannot give any density guarantee.

Kalaiah and Varshney [16] described a statistical-based geometry representation scheme, which can contribute to reduce network bandwidth and to high-quality interactive rendering without sacrificing visual realism. Nehab and Shilane [17] proposed a grid-based stratified sampling strategy for 3D models, which first voxelizes the underlying model and then selects one sample point for each voxel. However, these surface simplification approaches cannot sample the given 3D model to indicate its local geometric features exactly.

Due to the comprehensive research on mesh simplification [18–21], many greedy and local clustering mesh simplification schemes can be directly extended to point-sampled geometry. However, major difficulties for the direct extension are how to control the re-sampling density, and the approximation error for simplifying point-sampled geometry. Pauly et al. [7] adopted uniform incremental clustering and adaptive hierarchical clustering methods to simplify a given point cloud. The uniform incremental clustering approach is computationally efficient but is reported to cause high approximation error. Similarly, the hierarchical clustering approach is memory and execution efficient but even in its adaptive version the approximation error is not very low in general. Similar to the error-controlled mesh simplification scheme [18], Pauly et al. [7] also presented an iterative scheme to produce an optimal result in terms of average geometric accuracy. But it is not intuitive for the point set density control. Wu et al. [8] re-sample a given dense point set by a sparse set of circular or elliptical object-space splats. Nevertheless, the generation of initial splat candidates and guarantee of the simplified model of being free of holes are time-consuming.

Recently, particle simulation has become a popular approach for simplifying large-scale 3D models. Early in 1992, Turk [22] introduced a mesh re-sampling method via particle simulation. The particles with a specified number are randomly spread across the surface and they are approximately equal-distance distributed by using a point repulsion algorithm according to their curvature estimation. Witkin and Heckbert [23] used an adaptive repulsion and split-and-death criteria to scatter a particle system on an implicit surface which minimizes an energy criterion. Hart et al. [24] extended the method of Witkin and Heckbert to uniformly sample and control the more complex implicit surfaces. Pauly et al. [7] adopt particle simulation to simplify the point-sampled geometry by considering approximation accuracy and density controls. Recently, Proenca et al. [25] achieved non-uniform sampling MPU implicit surface according to the model features, i.e. high densities in the abundant feature areas and vice versa. In general, the particle simulation is a computationally demanding approach and is not efficient enough for the large-scale point-sampled models.

Local surface differentials estimation. In order to obtain the splats for each cluster produced by our technique, an important step of our algorithm is to estimate the local surface differentials. A detailed overview of surface differentials estimation algorithms can be found in recent papers [26,27] and the references therein.

Taubin [28] proposed a integral eigenvalue method to estimate the tensor of curvature using a one-ring neighborhood. Hameiri and Shimsoni [29] presented a modification of Taunbin's method by expanding to all the neighbor points inside a given radius across the normal sections for stable principal curvature estimate on discrete noisy range data. Applying the principal component analysis (PCA) method to the neighborhoods of sample points, Pauly et al. [7] proposed an algorithm to estimate normals and curvatures for point-sampled geometry. Translating from Taubin's method, Lange and Polthier [30] derived a similar method for estimating principal curvatures and principal curvature directions for point set surfaces.

The idea of surface fitting is always applied to estimate surface features. To calculate surface differentials analytically, the quadratic or cubic polynomial fitting is adopted to find an implicit representation that fits the geometry locally [31, 32]. Cazals and Pouget [33] proposed a method to estimate local surface differentials by polynomial fitting of an osculating jet. Rusinkiewicz [34] presented an algorithm to estimate the curvature tensor by least-squares fitting to the normal variations. Also using local least square fitting, Mitra et al. [35] described a method for estimating the normals at all sample points of a point cloud data set. Tong and Tang [36] proposed a tensor voting technique to robustly estimate curvature tensors. Based on Levin's moving least square (MLS) approximation method [37], Alexa and Adamson [38] adopted the gradient of the local implicit surface as an accurate surface normal estimate and presented efficient orthogonal projection operators for sampling theory. Based on the explicit definition for point-set surfaces [39], Yang and Qian [40] proposed a direct computing scheme for surface curvatures.

Recently, based on curvature tensor fitting, Kalogerakis et al. [26] proposed a robust statistical framework for curvature estimate on discretely sampled surfaces. Miao et al. [41] proposed a projection scheme to estimate local surface differentials for the point-sampled geometry. All of the sample points in the neighbors are projected onto the normal plane, and the two principal directions and curvatures can be obtained by normal curvature analysis regarding to only three sampled tangent directions.

In our implementation, we use the projection scheme [41] to estimate the principal directions and curvatures as it provides an efficient estimation of the principal directions and curvatures for point-set surfaces. However, our re-sampling method is not strictly dependent on this specific curvature estimate algorithm and other techniques also can be used instead.

Please cite this article in press as: Miao Y, et al. Curvature-aware adaptive re-sampling for point-sampled geometry. Computer-Aided Design (2009), doi:10.1016/j.cad.2009.01.006

3. Adaptive bandwidth mean-shift scheme

Based on the analysis of multi-modal feature space defined in both spatial and range domains, the mean-shift approach [42,43] is a powerful non-parametric feature space clustering technique for scattered point data. The geometric feature space itself can be regarded as an empirical probability density function, and the mean-shift scheme is a gradient ascend technique to search for the local maxima. Applying this scheme to each discrete point data set will create clusters around the maxima modes, which corresponds to a dense region in the feature space. Unlike many other parametric clustering techniques which take the number of the modes or clusters as a prerequisite, this scheme can determine them automatically by the mean-shift procedure itself.

Given a set of data points in spatial-range domain

$$\chi = \{X_i = (p_i, q_i) : p_i \in P \subseteq \mathbf{R}^{d_1},\ q_i \in Q \subseteq \mathbf{R}^{d_2}\},\quad i = 1, 2, \ldots, n$$

drawn from a density function $f(x) : \mathbf{R}^{d_1+d_2} \longmapsto \mathbf{R}$, we want to estimate the multivariate probability density at point x. In the definition of spatial-range domain $P \times Q$, the P represents the spatial position information for discrete data point set, while the Q denotes its range information, such as the normal information for sample points. The d_1 and d_2 are the dimensions of the spatial information and the range information, respectively. In order to handle the spatial and range intrinsic feature efficiently, the multivariate kernel density estimator can be divided into two parts, that is the spatial kernel $K_1(\cdot)$ and the range kernel $K_2(\cdot)$, and the density function can be estimated by

$$\hat{f}(p, q) = \frac{1}{n h_1^{d_1} h_2^{d_2}} \sum_{i=1}^{n} K_1\left(\frac{p - p_i}{h_1}\right) K_2\left(\frac{q - q_i}{h_2}\right)$$

where $K(x)$ is the so-called kernel function satisfying $\int_{R^d} K(x)\mathrm{d}x = 1$, the parameter h is a smoothing factor called the bandwidth. In general, the kernel function $K(x)$ is radially symmetric like $K(x) = ck(\|x\|^2)$, where $k(x)$ is called the profile function and c is a normalizing constant. Thus the separable multivariate density function becomes

$$\hat{f}(x) = \frac{c_1 c_2}{n h_1^{d_1} h_2^{d_2}} \sum_{i=1}^{n} k_1\left(\left\|\frac{p - p_i}{h_1}\right\|^2\right) k_2\left(\left\|\frac{q - q_i}{h_2}\right\|^2\right).$$

The mean-shift approach is considered as a gradient ascend search scheme for the maxima of a density function over the feature-space along the increasing direction of the function gradient. The gradient of density function can be deduced as

$$\nabla\hat{f}(x) = \frac{c_1 c_2}{n h_1^{d_1} h_2^{d_2}} \left(\frac{2}{h_1^2} \sum_{i=1}^{n} g_1\left(\left\|\frac{p - p_i}{h_1}\right\|^2\right) k_2\left(\left\|\frac{q - q_i}{h_2}\right\|^2\right)(p_i - p), \right.$$
$$\left. \frac{2}{h_2^2} \sum_{i=1}^{n} g_2\left(\left\|\frac{q - q_i}{h_2}\right\|^2\right) k_1\left(\left\|\frac{p - p_i}{h_1}\right\|^2\right)(q_i - q) \right)$$

where we denote $-k_1'(x)$ as $g_1(x)$, and $-k_2'(x)$ as $g_2(x)$ respectively.

Now, if we take the normal kernel $k(x) = \exp(-\frac{x}{\sigma^2})$, the shadow of the kernel becomes $g(x) = -k'(x) = ck(x)$. For the sake of alleviating the point data noise, the position σ and the normal σ are chosen as 3.0 and 10.0 respectively in our experiments, which can produce satisfied results in most cases. The advantages of the normal kernel is that the normal kernel and its shadow have the same expression except for a constant [43], that is,

$$\nabla\hat{f}(x) = \frac{c_1 c_2}{n h_1^{d_1} h_2^{d_2}} \left(\frac{2c}{h_1^2} \sum_{i=1}^{n} g_1\left(\left\|\frac{p - p_i}{h_1}\right\|^2\right) \right.$$
$$\left. \times g_2\left(\left\|\frac{q - q_i}{h_2}\right\|^2\right)(p_i - p), \right.$$
$$\left. \frac{2c}{h_2^2} \sum_{i=1}^{n} g_2\left(\left\|\frac{q - q_i}{h_2}\right\|^2\right) g_1\left(\left\|\frac{p - p_i}{h_1}\right\|^2\right)(q_i - q) \right).$$

Therefore, the local maxima of the density function can be obtained by solving the following equations:

$$\frac{\sum_{i=1}^{n} g_1(\|\frac{p-p_i}{h_1}\|^2) g_2(\|\frac{q-q_i}{h_2}\|^2)(p_i - p)}{\sum_{i=1}^{n} g_1(\|\frac{p-p_i}{h_1}\|^2) g_2(\|\frac{q-q_i}{h_2}\|^2)} = 0$$
$$\frac{\sum_{i=1}^{n} g_2(\|\frac{q-q_i}{h_2}\|^2) g_1(\|\frac{p-p_i}{h_1}\|^2)(q_i - q)}{\sum_{i=1}^{n} g_1(\|\frac{p-p_i}{h_1}\|^2) g_2(\|\frac{q-q_i}{h_2}\|^2)} = 0$$

or the fixed point of the iteration procedure,

$$I(p) = \frac{\sum_{i=1}^{n} g_1(\|\frac{p-p_i}{h_1}\|^2) g_2(\|\frac{q-q_i}{h_2}\|^2) p_i}{\sum_{i=1}^{n} g_1(\|\frac{p-p_i}{h_1}\|^2) g_2(\|\frac{q-q_i}{h_2}\|^2)} = p$$
$$I(q) = \frac{\sum_{i=1}^{n} g_2(\|\frac{q-q_i}{h_2}\|^2) g_1(\|\frac{p-p_i}{h_1}\|^2) q_i}{\sum_{i=1}^{n} g_1(\|\frac{p-p_i}{h_1}\|^2) g_2(\|\frac{q-q_i}{h_2}\|^2)} = q.$$

They can be solved by the mean-shift iteration.

In the fixed bandwidth mean-shift clustering scheme, the neighbor points within a fixed radius will depend heavily on the distribution of high-dimensional data points in the feature space, e.g. it maybe sparse or dense in the feature space. The sampling irregularity may lead to incorrect clustering results [44]. In our adaptive mean-shift clustering, for each data point p in the d-dimensional feature space R^d, a key step is to determine a proper size of neighborhood $N(p)$ and the associated adaptive bandwidth value $h(p)$ through following equation,

$$h(p) = \max_{q \in N(p)} (dist(p, q))$$

that is, the maximum distance between data point and its neighbors.

For each sample point, the traditional k-nearest neighborhoods only consider their position information and neglects their normal variance. One potential solution to this issue is an adaptive neighbor selection, which reflects both the position information and normal variance around sample points. For each sample point p, the traditional neighborhood N_k is defined by k-nearest neighbors. Then, depending on the local sampling density and local feature size at the sample point, the normals of the neighboring points $q \in N_k$ can span quite a different range, that is, the bounding cone-of-normals of all normals of the points $q \in N_k$ is not constant for a k-nearest neighborhood. Our adaptive neighbors of sample point p can be selected as all points q in N_k within a certain angle of normal deviation. These neighbors span a (bounding) normal cone of a pre-defined opening angle. In our implementation, the parameter k for the initially chosen neighborhood N_k and the angle of bounding cone for obtaining the final adaptive neighborhood are selected as 16 and 15°, respectively, which work well in our experimentation. Therewith, the size of neighbors of each point is about 6–16, that is, it ranges adaptively from 6 to 16. In fact, the selection of the neighborhood size of each sample point is not a determinant for our re-sampling results. Fig. 1 illustrates

Please cite this article in press as: Miao Y, et al. Curvature-aware adaptive re-sampling for point-sampled geometry. Computer-Aided Design (2009), doi:10.1016/j.cad.2009.01.006

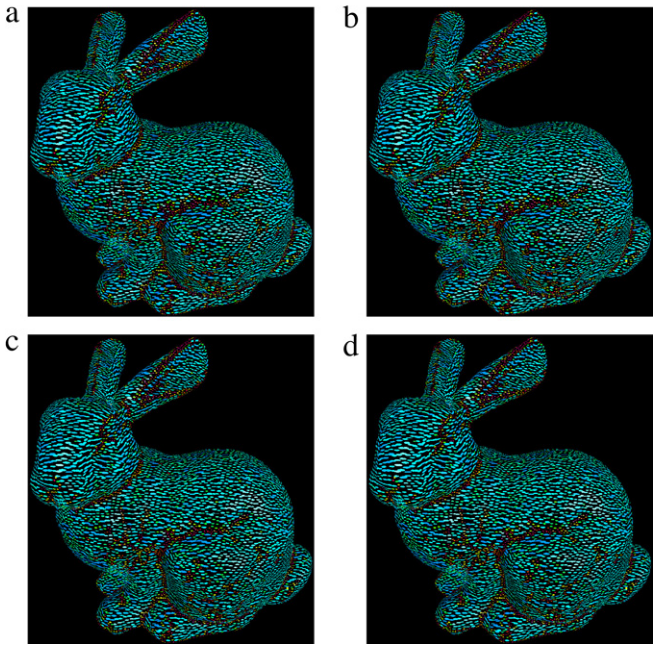

Fig. 1. Our adaptive re-sampling results in terms of different neighbor selections, whereas the weights for position and normal variation are always chosen as (0.2, 0.8). (a) The size of neighbors of each point is about 6–16, whilst the number of simplified points is 16 729; (b), (c) and (d) The size of neighbors of each point is 12–16, 6–24 and 12–24, respectively, whilst the number of simplified points is 16 728, 16 546 and 16 553, respectively.

the different re-sampling results in terms of different selections of neighborhood size.

To find the local maxima mode by mean-shift iteration, we first calculate the weighted average of the data points that fall inside this neighboring window, and then iteratively move the window to the mean point. The weighted mean at a feature data point p in the joint feature space is defined by a monotonically decreasing symmetric profile Gaussian kernel $g(x)$ with the adaptive radius $h(p)$ in the feature space. The mean shift local maxima mode in the feature space can be evaluated by the following iteration procedure:

$$M_h^v(p) := \frac{\sum_{i=1}^{n} g_1(\|\frac{p-p_i}{h_1}\|^2) g_2(\|\frac{q-q_i}{h_2}\|^2) p_i}{\sum_{i=1}^{n} g_1(\|\frac{p-p_i}{h_1}\|^2) g_2(\|\frac{q-q_i}{h_2}\|^2)} - p$$

$$p^{t+1} := p^t + M_h^v(p^t);$$

$$M_h^v(q) := \frac{\sum_{i=1}^{n} g_2(\|\frac{q-q_i}{h_2}\|^2) g_1(\|\frac{p-p_i}{h_1}\|^2) q_i}{\sum_{i=1}^{n} g_1(\|\frac{p-p_i}{h_1}\|^2) g_2(\|\frac{q-q_i}{h_2}\|^2)} - q$$

$$q^{t+1} := q^t + M_h^v(q^t),$$

where the convergent point p^* of the above mean-shift iterative procedure is also called the mean-shift local mode, in which the initial value can coincide with p and $M_h^v(p)$ is the mean-shift vector associated with the adaptive bandwidth.

4. Adaptive re-sampling for point-sampled geometry

In surface data acquisition, the modern 3D scanning devices are capable of producing point clouds that contain millions of sample points. These sample points are often converted into a continuous surface representation for further graphics and geometry processing. Many of these conversion algorithms are computationally expensive and require substantial amounts of main memory. Reducing the complexity of such data sets is one of the key preprocessing steps for subsequent applications, such as point-based modeling, real-time rendering and visualization, etc.

Owing to the above mean-shift iterative scheme for discrete sample points, the corresponding mean-shift local modes can be determined. In Section 4.1, we present our hierarchical clustering scheme to reduce the complexity of large data sets based on their mean-shift local modes. Then, in Section 4.2, we explain how to obtain the representative splats for each cluster based on the fast projection and curvature estimation method of [41].

4.1. Hierarchical clustering for local maxima modes

It is argued that effective surface simplification can be performed in the feature space, similar to other point-based processing and visualization applications. We adopt a hierarchical clustering approach to simplify the input point-sampled geometry. For each sample point, a corresponding mean-shift local mode can be calculated according to the above iterative procedure. The sample points with the approximately same mean-shift local modes are clustered hierarchically. Applying our scheme to a set of given discrete data points will create some clusters around the maxima modes, which correspond to the dense distribution regions in the feature space. The set of local modes will be split if one of the following criteria is satisfied:

- the size of the set with local maxima modes is larger than a user specified maximum cluster size, or
- the variation within a set of local modes is above a given threshold.

In our implementation, the user specified maximum cluster is selected as 30 sample points. The local modes variation information can be obtained by the covariance analysis method, which is composed of two parts, i.e., the position variation $\Delta_{position}$ and the normal variation Δ_{normal}. Finally the definition of local modes variation is the linear combination of them:

$\omega_{position}\Delta_{position} + \omega_{normal}\Delta_{normal}$.

If the splitting criterion is not satisfied, the set of local modes becomes a cluster. Thus, we can build a binary tree, and each leaf node corresponds to a cluster. The sampling points in each cluster are abstracted as a representative splat, and a simplified geometry is created.

4.2. Representing surface splat elements

For each cluster, the representative splat can be obtained by the principal component analysis approach [7,8,45]. The position of splat is chosen as the centroid of the sampling points in the cluster and its normal direction is chosen as the eigenvector associated with the minimal eigenvalue of the covariance matrix of the sampling points in the cluster. Then, using our projection scheme to local surface differentials estimation for the point-sampled geometry [41], all sampling points in the cluster are projected to the normal plane at the splat, and the two principal directions are obtained by normal curvature analysis regarding to only three sampled tangent directions. Finally, to render the simplified sample point efficiently, an elliptic splat is adopted to address the anisotropic sampling property as [8], in which the principal curvatures and principal directions are chosen to fully determine the elliptic splat.

5. Results and discussion

All the algorithms presented in this paper are implemented and tested on a PC with a Pentium IV 3.0 GHz CPU, 1024M memory.

Please cite this article in press as: Miao Y, et al. Curvature-aware adaptive re-sampling for point-sampled geometry. Computer-Aided Design (2009), doi:10.1016/j.cad.2009.01.006

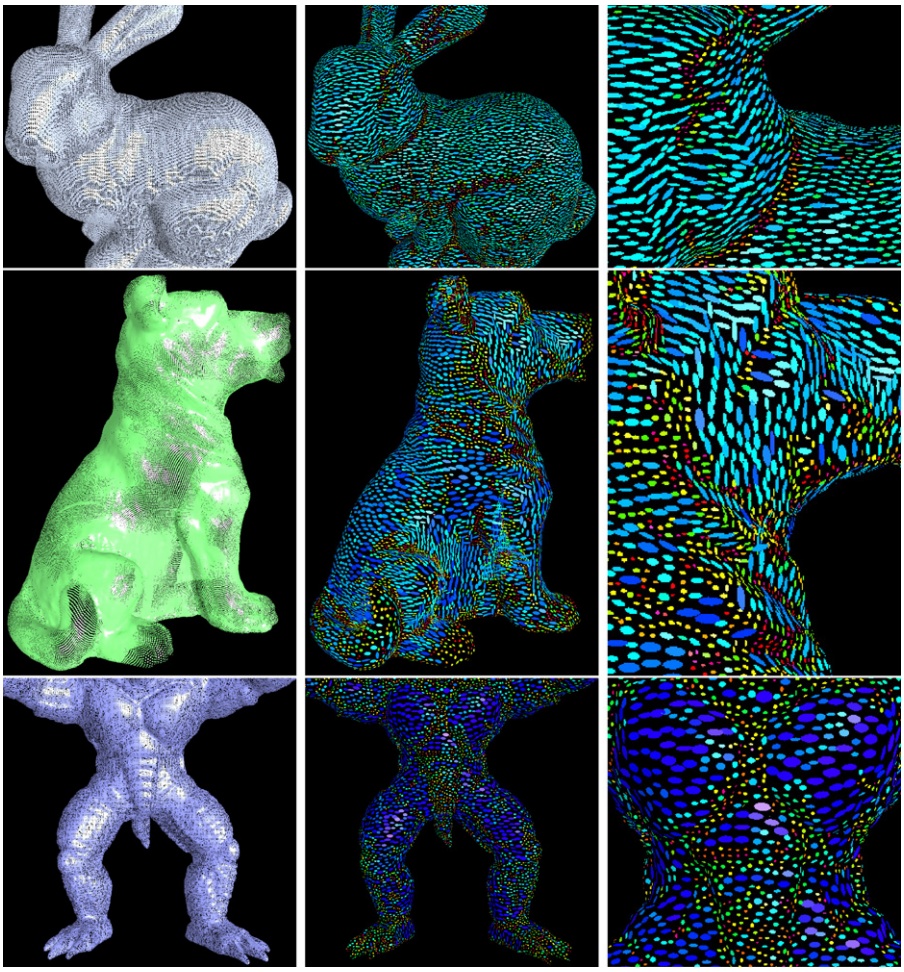

Fig. 2. Adaptive re-sampling by point position and normal information. Left column: The original sampling for different models. Middle column: Color maps for the results of adaptive re-sampling different models by point position and normal information, in which different colors show the different sizes of clusters, that is, the pink means small size of cluster, and blue means large size of clusters, etc. Right column: The zoom-in views of the corresponding sampling results.

In our mean-shift clustering algorithm, the feature space definition and the clustering criteria of local modes are very important to the final simplification result. During the mean-shift local modes clustering, the local modes variation will affect the clustering results, which could be adjusted by selecting different weights for the position variation and the normal variation.

5.1. Adaptive re-sampling via position and normal attributes

In general, surface normal gives us first order information of the underlying surface variation around the sample point, and the variation of normal direction can reflect the curvature distribution to some extent. In order to adaptively sample the surface according to the curvature variation, it should perform clustering algorithm in the combinative spatial and range domains, i.e. position and normal information for each sample point.

Fig. 2 gives three re-sampling examples. In these examples, the threshold for mean-shift clustering is 0.10, and all weights for the local modes variations are the same, i.e. $(\omega_{position}, \omega_{normal}) = (0.2, 0.8)$. The results illustrate that the proposed re-sampling scheme is a curvature aware manner, i.e. the simplification points at the high curvature regions are dense, while those at the planar low curvature regions are sparse.

Using the same threshold and weights for mean-shift clustering as Fig. 2, Fig. 3 gives another two re-sampling results for raw scanned point clouds. The experiments show that our re-sampling results can reflect the curvature distribution of the underlying models even for non-uniformly sampled dragon model and for noisy Max-Planck model.

5.2. Adjusting the sampling density of simplified model

In our proposed framework, the sampling density could be adjusted easily to satisfy different requirements of the simplified model. The sampling density can be adjusted by two different ways. One is the threshold for mean-shift clustering, and the other is the weights for position and normal variation.

Different thresholds in mean-shift clustering can generate different re-sampling results. Fig. 4 shows the experimental results by setting different thresholds in our clustering procedure for Stanford bunny model simplification. If the threshold is chosen as 0.10 for mean-shift clustering, the number of sampling points in the simplified model is 16 729, while it is 23 304 for the threshold 0.05. However, if the threshold is chosen as 0.20 for mean-shift clustering, the number of sampling points in the simplified model is 14 381. The experimental results show that large threshold will lead to small number of the sampling points in final simplified model, but they can reflect the surface intrinsic curvature distribution.

Moreover, the sampling density could also be changed and adjusted through adjusting the weights $\omega_{position}$ and ω_{normal}. Fig. 5 illustrates the different re-sampling results by choosing different weights. The number of sampling points for the simplified model is highly correlative with the selected weights for the mean-shift

Please cite this article in press as: Miao Y, et al. Curvature-aware adaptive re-sampling for point-sampled geometry. Computer-Aided Design (2009), doi:10.1016/j.cad.2009.01.006

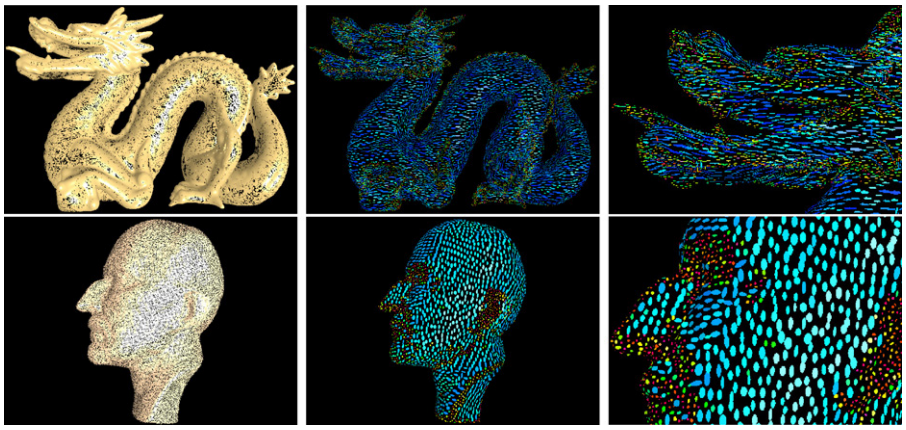

Fig. 3. Adaptive re-sampling by point position and normal information. First row: The original non-uniform sampling and our adaptive re-sampling result for dragon model. Second row: The original sampling and the adaptive re-sampling result for noisy Max-Planck model.

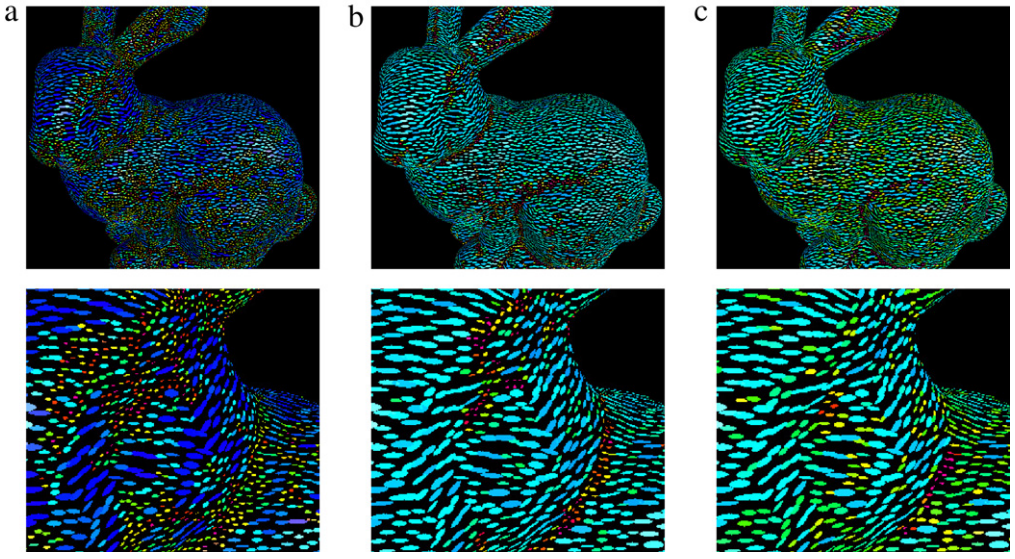

Fig. 4. Adaptive re-sampling by selecting different thresholds for mean-shift clustering, whereas the weights for position and normal variation are always chosen as (0.2, 0.8). (a), (b) and (c) The thresholds for clustering are 0.05, 0.10 and 0.20, respectively. Below row is the zoom-in views of the corresponding sampling results.

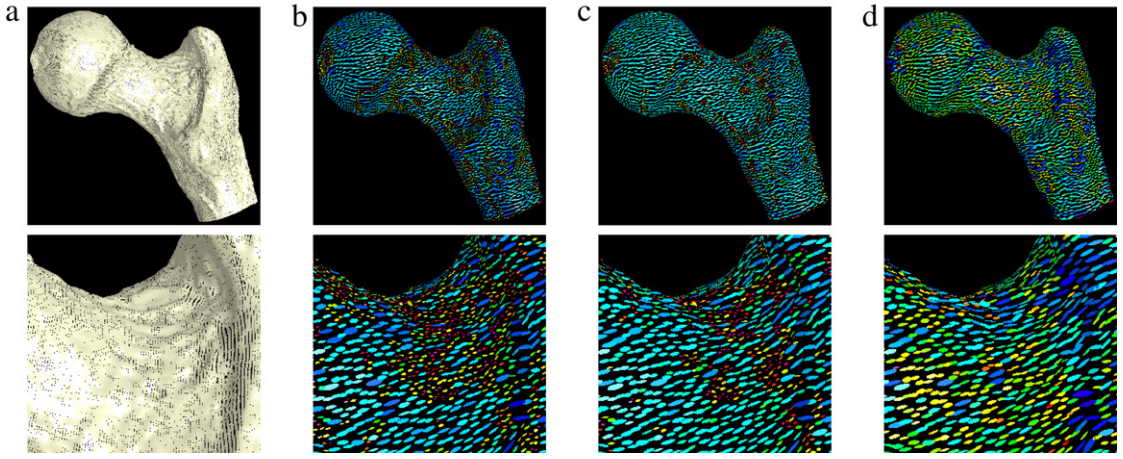

Fig. 5. Adaptive re-sampling by selecting different weights for position and normal variation for mean-shift clustering, whereas the threshold is always chosen as 0.10. (a) Original sampling for balljoint model; (b), (c), (d) The re-sampling results by selecting different weight for mean-shift clustering, that is, the weights for position and normal variation are (0.2, 0.8), (0.5, 0.5), and (0.8, 0.2), respectively. Below row is the zoom-in views of the corresponding sampling results.

clustering. For example, for balljoint model (the original number of sample points is 137 062), if the weights for position and normal variation are (0.2, 0.8), the number of sampling points in the simplified model is 9857, while it is 7062 for the weights (0.8, 0.2)

Please cite this article in press as: Miao Y, et al. Curvature-aware adaptive re-sampling for point-sampled geometry. Computer-Aided Design (2009), doi:10.1016/j.cad.2009.01.006

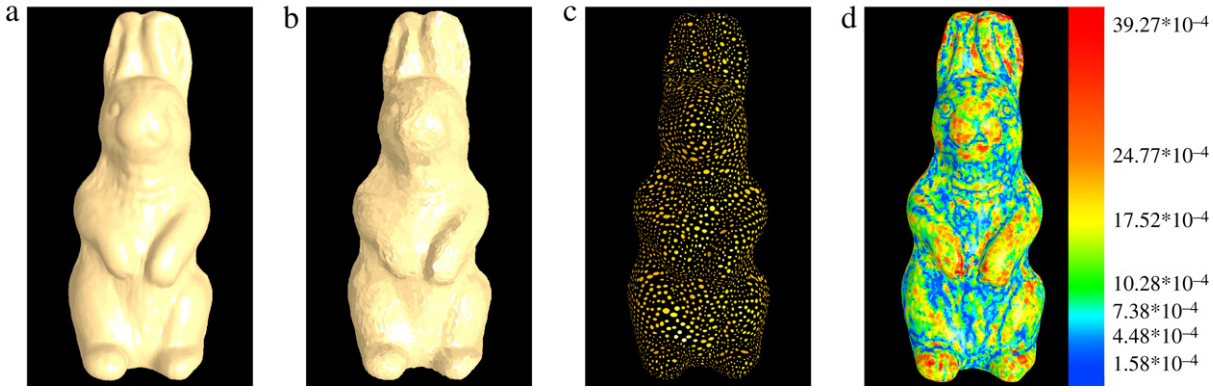

Fig. 6. Geometric error analysis for the simplified rabbit model. (a) and (b) The original model and simplified one; (c) Re-sampling results by selecting the weights for position and normal variation as (0.2, 0.8) and (d) the color map of geometric error for simplified model, in which different colors show the different magnitudes of normalized error at simplified sample points.

Table 1
Time statistics of the proposed simplification and re-sampling scheme for different point-sampled models. The time data are collected on a PC with a Pentium IV 3.0 GHz CPU, 1024M memory.

Models	#Points	Timings for different stages			#Points of simplified model	Normalized average error Δ^*_{avg}
		Differential estimation (s)	Mean-shift iteration (s)	Mean-shift clustering (s)		
Dragon	437 645	3.93	38.16	11.51	34 049	5.29×10^{-4}
Bunny	280 792	2.55	15.01	2.73	16 729	4.73×10^{-4}
Dog	195 586	1.77	11.97	1.92	14 159	6.31×10^{-4}
Armadillo	172 974	1.51	9.56	1.67	15 482	8.24×10^{-4}
Balljoint	137 062	1.24	6.92	1.29	9 857	6.54×10^{-4}
Noisy Planck	96 844	0.86	4.04	2.49	5 873	11.14×10^{-4}
Santa	75 781	0.67	5.05	0.65	6 983	9.90×10^{-4}
Rabbit	67 038	0.60	3.16	0.58	4 493	10.28×10^{-4}

and it is 8485 for the weights (0.5, 0.5). Our experimental results also show that the sampling result using a large ω_{normal} will reflect the surface intrinsic curvature distribution, whilst a large $\omega_{position}$ will lead to a uniform sampling.

5.3. Geometric error analysis by our re-sampling scheme

To evaluate the quality of the simplified geometry generated by our re-sampling algorithm, some methods should be introduced to measure the geometric error between original and simplified version of the given model. Similar to the 3D mesh Metro analysis tool [46,7], we measure the geometric error as both the maximum error between original version S and simplified model S', i.e. the Hausdorff distance,

$$\Delta_{\max}(S, S') = \max_{q \in S} d(q, S')$$

and geometric average error, i.e.,

$$\Delta_{\text{avg}}(S, S') = \frac{1}{\|S\|} \sum_{q \in S} d(q, S'),$$

respectively. The corresponding normalized geometric errors can then be obtained by scaling the above error measures according to the model's bounding box diagonal.

For each sample point $q \in S$, the geometric error $d(q, S')$ can then be defined as the Euclidean distance between the sample point q and its projection point $\bar{q}$ on the simplified surface S'. This projection point can be obtained by the simple "almost" orthogonal projection approach [38].

Fig. 6 shows the solid rendering of the simplified model and the color map of geometric error for the rabbit model that has been simplified from 67 038 points to 4493 points (the weights for position and normal variation are 0.2 and 0.8 for mean-shift clustering, the threshold is 0.10). The normalized average geometric error is $\Delta^*_{\text{avg}} = 10.28 \times 10^{-4}$, while the normalized max geometric error is $\Delta^*_{\max} = 0.0062$.

Table 1 shows the data and time statistics for the example models and algorithms in this paper. For example, the total number of sample points for the Stanford bunny model is 280 792, while the number of sample points for simplified model is 16 729. The timings for differential estimation, Mean-shift iteration, and Mean-shift clustering are 2.55 s, 15.01 s, and 2.73 s, respectively. The normalized average error is $\Delta^*_{\text{avg}} = 4.73 \times 10^{-4}$. This table illustrates the efficiency of our adaptive re-sampling scheme.

In Fig. 7, we compare our curvature-aware re-sampling scheme with Pauly et al. [7] clustering approaches for point-sampled geometry simplification. It shows the quantitative error estimates (scaled according to the object's bounding box diagonal) for the Stanford bunny model that has been simplified as 6% of original points. Uniform incremental clustering has the highest average geometric error and adaptive hierarchical clustering performs slightly better. However, our curvature-aware mean-shift re-sampling scheme provides lower geometric error, comparing with the uniform incremental and adaptive hierarchical clustering schemes.

6. Conclusions and future work

A novel curvature aware re-sampling approach is proposed, which is based on an adaptive mean-shift clustering scheme. The proposed re-sampling scheme can adaptively reflect the intrinsic property of the underlying 3D model, which leads to a non-uniform sampling distribution and can account for the local geometric features in a curvature-aware manner. That is, the sample points

Please cite this article in press as: Miao Y, et al. Curvature-aware adaptive re-sampling for point-sampled geometry. Computer-Aided Design (2009), doi:10.1016/j.cad.2009.01.006

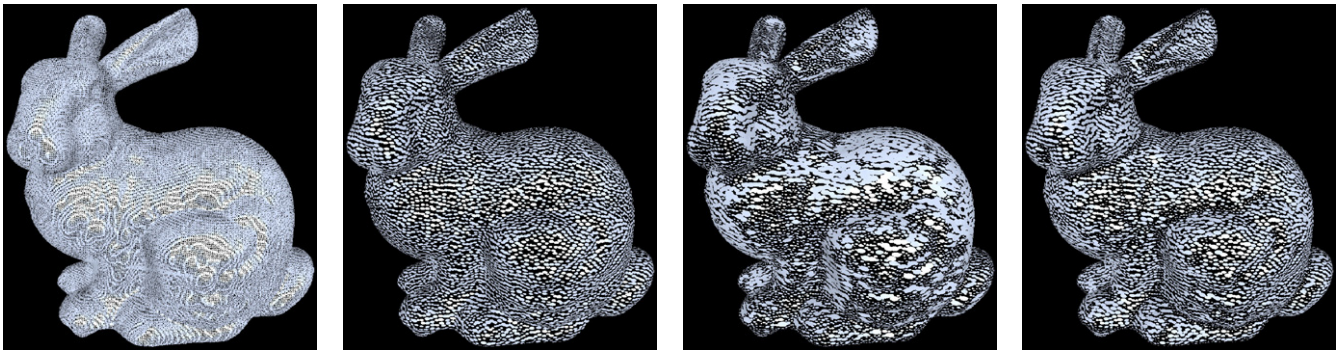

(a) Original sampling. (b) $\Delta^*_{avg} = 5.27 \times 10^{-4}$, $\Delta^*_{max} = 0.0098$. (c) $\Delta^*_{avg} = 4.81 \times 10^{-4}$, $\Delta^*_{max} = 0.0053$. (d) $\Delta^*_{avg} = 4.73 \times 10^{-4}$, $\Delta^*_{max} = 0.0096$.

Fig. 7. The re-sampling results and geometric error comparisons via different clustering simplification schemes. (a) Original sampling for Stanford bunny model; (b) Re-sampling result by uniform incremental clustering scheme; (c) Re-sampling result by adaptive hierarchical clustering scheme; (d) Re-sampling result by our curvature-aware mean-shift re-sampling scheme. The number of simplified points is 6% of original points for three simplification schemes.

are dense in the high curvature regions, while they are sparse in the planar low curvature regions.

However, it is difficult to incorporate the simplified geometric error in our adaptive mean-shift clustering algorithm. One possible solution maybe simplify point clouds according to an user-defined error threshold, that is, control sample points generation of the target model under specifying geometric error bounds. Whereas the surface sampling size should be proportional to the total absolute Gaussian curvature [47], we can use the Gaussian sphere to approximate this curvature and control the approximation error by the sampling on the Gaussian sphere. For the current algorithm, it is also difficult to give an intuitive user-specified parameter to adjust the re-sampling result. Because the variation threshold is based on the combination of position variation and normal variation, we cannot find its intuitive meaning at present. Maybe we can consider it as future work.

Therefore, the future research should focus on the Gaussian sphere based sampling, the introduction of an intuitive parameter, and some related geometry processing, such as model compression, streaming processing, etc.

Acknowledgements

We would like to thank the anonymous reviewers for their valuable comments. This research work is supported by the State Scholarship Fund of China. This work is also partly supported by the National Natural Science Foundation of China under Grant Nos. 60743002, 60736019 and the Natural Science Foundation of Zhejiang Province under Grant Nos. Y107311, R106449.

References

[1] Levoy M, Pulli K, Curless B, Rusinkiewicz S, Koller D, Pereira L. et al. The digital michelangelo project: 3d scanning of large statues. In: Proceedings of ACM SIGGRAPH. 2000. p. 131–144.
[2] Linsen L. Point cloud representation. Tech. report 2001-3. Germany: Computer Science Dept., Universitaet Karlsruhe; 2001. http://www.math-inf.uni-greifswald.de/~linsen/publications/Linsen01a.pdf.
[3] Gross M, Pfister H, editors. Point-based graphics. Series in computer graphics, Morgan Kaufmann Publishers; 2007.
[4] Alexa M, Behr J, Cohen-or D, Fleishman S, Levin D, Silva CT. Computing and rendering point set surfaces. IEEE Transactions on Visualization and Computer Graphics 2003;9(1):3–15.
[5] Pauly M, Keiser R, Kobbelt L, Gross M. Shape modeling with point-sampled geometry. ACM Transactions on Graphics 2003;22(3):641–50.
[6] Zwicker M, Pauly M, Knoll O, Gross M. Pointshop 3d: An interactive system for point-based surface editing. ACM Transactions on Graphics 2002;21(3):322–9.
[7] Pauly M, Gross M, Kobbelt L. Efficient simplification of point-sampled surfaces. In: Proceedings of IEEE visualization 2002. 2002. p. 163–170.
[8] Wu JH, Kobbelt L. Optimized sub-sampling of point sets for surface splatting. Computer Graphics Forum 2004;23(3):643–52.
[9] Amenta N, Choi S, Kolluri R. The power crust. In: Solid modeling. 2001. p. 249–60.
[10] Dey TK, Giesen J, Goswami S, Zhao W. Shape dimension and approximation from samples. In: Proceedings of 13th ACM SIAM sympos. discrete algorithms. 2002. p. 772–780.
[11] Gopi M. On sampling and reconstructing surfaces with boundaries. In: Canadian conference on computational geometry. Lethbridge (Canada); 2002. p. 49–53.
[12] Weyrich T, Pauly M, Keiser R, Heinzle S, Scandella S, Gross M. Post-processing of scanned 3D surface data. In: Eurographics symposium on point-based graphics. Zurich; 2004. p. 85–94.
[13] Dey TK, Giesen J, Hudson J. Decimating samples for mesh simplification. In: Proc. 13th Canadian conference on computational geometry. 2001. p. 85–88.
[14] Moenning C, Dodgson NA. A new point cloud simplification algorithm. In: Proceedings of the 3rd international conference on visualization, imaging and image processing. 2003. p. 1027–33.
[15] Moenning C, Dodgson NA. Intrinsic point cloud simplification. In: Proceedings of the 14th international conference on computer graphics and vision. 2004. p. 1147–54.
[16] Kalaiah A, Varshney A. Statistical point geometry. In: Eurographics symposium on geometry processing. 2003. p. 107–15.
[17] Nehab D, Shilane P. Stratified point sampling of 3d models. In: Eurographics symposium on point-based graphics. Zurich; 2004. p. 49–56.
[18] Garland M, Heckbert P. Surface simplification using quadric error metrics. In: Proceedings of ACM SIGGRAPH. 1997. p. 209–16.
[19] Garland M, Willmott A, Heckbert P. Hierarchical face clustering on polygonal surfaces. In: Proceedings of ACM symposium on interactive 3D graphics. 2001. p. 49–58.
[20] Katz S, Tal A. Hierarchical mesh decomposition using fuzzy clustering and cuts. ACM Transaction on Graphics 2003;22(3):954–61.
[21] Yamauchi H, Lee S, Lee Y, Ohtake Y, Belyaev A, Seidel H-P. Feature sensitive mesh segmentation with mean shift. In: International conference on shape modeling and applications. Washington (DC, USA); 2005. p. 238–45.
[22] Turk G. Re-tiling polygonal surfaces. In: Proceedings of ACM Siggraph. 1992. p. 55–64.
[23] Witkin AP, Heckbert PS. Using particles to sample and control implicit surfaces. In: Proceedings of ACM SIGGRAPH. 1994. p. 269–78.
[24] Hart JC, Bachta E, Jarosz W, Fleury T. Using particles to sample and control more complex implicit surfaces. ACM SIGGRAPH 2005 courses.
[25] Proenca J, Jorge JA, Sousa MC. Sampling point-set implicits. In: Proceedings of eurographics symposium on point-based graphics. 2007. p. 11–8.
[26] Kalogerakis E, Simari P, Nowrouzezahrai D, Singh K. Robust statistical estimation of curvature on discretized surfaces. In: Proceedings of the fifth eurographics symposium on geometry processing. 2007. p. 13–22.
[27] Gatzke T, Grimm C. Estimating curvature on triangular meshes. International Journal of Shape Modeling 2006;12(1):1–29.
[28] Taubin G. Estimating the tensor of curvature of a surface from a polyhedral approximation. In: Fifth international conference on computer vision'95. 1995. p. 902–7.
[29] Hameiri E, Shimsoni I. Estimating the principal curvatures and the Darboux frame from real 3D range data. IEEE Transactions on Systems, Man, and Cybernetics 2003;33(4):626–37.
[30] Lange C, Polthier K. Anisotropic smoothing of point sets. Computer Aided Geometric Design 2005;22(7):680–92.
[31] Meek DS, Walton DJ. On surface normal and gaussian curvature approximations given data sampled from a smooth surface. Computer Aided Geometric Design 2000;17(6):521–43.
[32] Goldfeather J, Interrante V. A novel cubic-order algorithm for approximating principal direction vectors. ACM Transaction on Graphics 2004;23(1):45–63.
[33] Cazals F, Pouget M. Estimating differential quantities using polynomial fitting of osculating jets. In: Eurographics symposium on geometry processing. 2003. p. 177–87.

Please cite this article in press as: Miao Y, et al. Curvature-aware adaptive re-sampling for point-sampled geometry. Computer-Aided Design (2009), doi:10.1016/j.cad.2009.01.006

[34] Rusinkiewicz S. Estimating curvatures and their derivatives on triangle meshes. In: Proceedings of the 3D data processing visualization and transmission. 2004. p. 486–93.
[35] Mitra NJ, Nguyen A, Guibas L. Estimating surface normals in noisy point cloud data. International Journal of Computational Geometry and Applications 2004; 14:261–76 [special issue].
[36] Tong W-S, Tang C-K. Robust estimation of adaptive tensors of curvature by tensor voting. IEEE Transactions on Pattern Analysis and Machine Intelligence 2005;27(3):434–49.
[37] Levin D. Mesh-independent surface interpolation. In: Brunnett G, Hamann B, Mueller K, Linsen L, editors. Geometric modeling for scientific visualization. Springer-Verlag; 2003. p. 37–49.
[38] Alexa M, Adamson A. On normals and projection operators for surfaces defined by point sets. In: Eurographics symposium on point-based graphics'04. Zurich; 2004. p. 149–155.
[39] Amenta N, Kil Y. Defining point-set surfaces. ACM Transactions on Graphics 2004;23(3):264–70.
[40] Yang P, Qian X. Direct computing of surface curvatures for point-set surfaces. In: Eurographics symposium on point-based graphics. 2007. p. 29–36.
[41] Miao Y, Feng J, Xiao C, Peng Q, Forrest A. Differentials-based segmentation and parameterization for point-sampled surfaces. Journal of Computer Science and Technology 2007;22(5):749–60.
[42] Comaniciu D, Meer P. Mean shift analysis and applications. In: Proceedings of IEEE international conference on computer vision. 1999. p. 186–96.
[43] Comaniciu D, Meer P. Mean shift: A robust approach toward feature space analysis. IEEE Transactions Pattern Analysis and Machine Intelligence 2002; 24(5):603–19.
[44] Georgescu B, Shimshoni I, Meer P. Mean shift based clustering in high dimensional: A texture classification example. In: Proceedings of international conference on computer vision. 2003. p. 456–63.
[45] Pajarola R, Sainz M, Guidotti P. Confetti: Object–space point blending and splatting. IEEE Transactions on Visualization and Computer Graphics 2004; 10(5):598–608.
[46] Cignoni P, Rocchini C, Scopigno R. Metro: Measuring error on simplified surfaces. Computer Graphics Forum 1998;17(2):167–74.
[47] Clarkson KL. Building triangulations using ε-nets. In: Proceedings of the thirty-eighth annual ACM symposium on theory of computing. 2006. p. 326–35.

Please cite this article in press as: Miao Y, et al. Curvature-aware adaptive re-sampling for point-sampled geometry. Computer-Aided Design (2009), doi:10.1016/j.cad.2009.01.006